

Effect of viscosity in the dynamics of two point vortices: Exact results

Olivier Agullo*

Physique des Interactions Ioniques et Moleculaire, UMR 6633, Équipe Dynamique des Systèmes Complexes, CNRS, Université de Provence,

Centre Universitaire de Saint-Jérôme, F-13397 Marseille Cedex 20, France

Alberto Verga†

Institut de Resherche sur les Phenomenes Hors Equilibre, UMR 6594, CNRS, Université de Provence, 49, rue F. Joliot-Curie, BP 146, 13384 Marseille, France

(Received 24 March 2000; published 13 April 2001)

An exact, unstationary, two-dimensional solution of the Navier-Stokes equations for the flow generated by two point vortices is obtained. The viscosity ν is introduced as a Brownian motion in the Hamiltonian dynamics of point vortices. The point vortices execute a stochastic motion whose probability density can be computed from a Fokker-Planck equation, equivalent to the original Navier-Stokes equation. The derived solution describes, in particular, the merging process of two Lamb vortices, and the development of the characteristic spiral structure in the topology of the vorticity. The viscous effects are thoroughly investigated by an asymptotic analysis of the solution. In particular, the selection mechanism of a specific pattern among the infinity satisfying the $\nu=0$ (Euler) equation is discussed.

DOI: 10.1103/PhysRevE.63.056304

PACS number(s): 47.52.+j, 47.27.Qb, 05.40.-a, 76.90.+d

I. INTRODUCTION

Vortex interaction is a central issue in two-dimensional fluid turbulence [1–3]. The basic mechanism, the collision of two localized vortices, was studied extensively, mainly using numerical simulations [4,5], in an attempt to understand the dynamics of coherent structures. Asymptotic analysis also contributed to the study of the motion of vortices in a two-dimensional potential flow, and the results were used to design efficient numerical schemes and describe the merging process [6,7]. A fundamental point about vortex interactions is the appearance of a spiral structure, evolving rapidly and contributing to the generation of small scales. The spiral structure is often invoked to explain the statistical properties of turbulence [8–12]. In this paper we show that using a stochastic representation of the Navier-Stokes equations, it is possible to find the exact solution for the interaction of two vortices in the limit of vanishing core size. The role of the viscosity and the detailed description of the spiral structure are thoroughly investigated.

In Euler flows, point vortices follow the fluid streamlines. This is no longer the case in viscous flows where, indeed, the viscosity perturbs this characteristic (advective) behavior. To give a more precise idea of the influence of viscosity on the vortices, let us introduce the Navier-Stokes equation for the vorticity in two-dimensional flow \mathbb{R}^2 ,

$$\left(\frac{\partial}{\partial t} + \mathbf{v} \cdot \nabla\right) \omega = \nu \nabla^2 \omega, \quad (1.1)$$

which can be completed with the incompressibility condition $\nabla \cdot \mathbf{v} = 0$. We note that ν is the kinematic viscosity, $\mathbf{v} = \mathbf{v}(x, t)$ is the velocity field, and $\omega = \omega(\mathbf{x}, t)$ is the algebraic

value of the vorticity $\boldsymbol{\omega} = \nabla \times \mathbf{v}$. In two-dimensional flows, the vorticity vector is in the direction perpendicular to the flow plane. Units are such that the constant fluid density is equal to 1. Solutions of this equation are smooth fields of the vorticity. To work with singular distribution of vorticity, it is more appropriate to introduce a weak form of the Navier-Stokes equation [Eq. (1.1)],

$$\frac{d}{dt} \omega_t(f) = \omega_t(\mathbf{v} \cdot \nabla f) + \nu \omega_t(\nabla^2 f), \quad (1.2)$$

for any smooth function f , where by definition $\omega_t(f) = \int_{\mathbb{R}^2} d\mathbf{x} \omega(\mathbf{x}, t) f(\mathbf{x})$. One should note that a weak solution [Eq. (1.2)] of the Navier-Stokes equation is not necessarily a solution of Eq. (1.1) that is to say a strong solution. Nevertheless, Eq. (1.2) is valid in a more general space of functions than the usual one [Eq. (1.1)], and allows one to deal with singular vorticity distributions rigorously. An important result follows from this approach in the case, where $\omega_t(f)$ is essentially bounded and integrable: one can associate a stochastic process $\mathbf{x}(t; \mathbf{x}_0)$ with any weak solution of the Navier-Stokes equations $\omega_t(f)$ defined by a Langevin equation [13]

$$\frac{d\mathbf{x}(t)}{dt} = \mathbf{v}[\mathbf{x}(t), t] + \sqrt{2\nu} \mathbf{b}(t), \quad (1.3)$$

$$\omega_t(f) = \int d\mathbf{x}_0 \omega(\mathbf{x}_0, 0) \mathcal{E}[f(\mathbf{x}(t; \mathbf{x}_0))], \quad (1.4)$$

where $\omega(\mathbf{x}_0, 0)$ is the initial vorticity field, \mathbf{b} is a white noise (the derivative of a Wiener process) and $\mathcal{E}(f)$ is the expected value of the stochastic process $f(\mathbf{x}(t; \mathbf{x}_0))$. By definition, $\mathcal{E}[f(\mathbf{x}(t; \mathbf{x}_0))] = \int d\mathbf{x} P(\mathbf{x}, t; \mathbf{x}_0) f(\mathbf{x})$, where $P(\mathbf{x}, t; \mathbf{x}_0)$ is the transition probability, that is, the probability for a particle, evolving according to process (1.3), and initially at position \mathbf{x}_0 , to be at position \mathbf{x} at time t . Equation (1.3) clearly shows that the viscosity prevents the advection of particles along the field lines by imposing a stochastic perturbation. Indeed,

*Electronic address: agullo@up.univ-mrs.fr

†Electronic address: verga@marius.univ-mrs.fr

in the absence of viscosity, Eq. (1.3) represents the motion of a fluid particle in the so called Lagrange representation of fluid motion.

The stochastic equation [Eq. (1.3)] is not very useful in this form, because to determine the fluid particle trajectory $\mathbf{x}(t)$ one needs to determine the velocity field $\mathbf{v}(\mathbf{x},t)$ which is itself a solution of the Navier-Stokes equation. However, in the special case where the vorticity is concentrated in points, an explicit form of the stochastic equation of motion for these ‘‘point vortices’’ can be found.

In the absence of viscosity, the Navier-Stokes equation reduces to a Euler equation. A weak version of the Euler equation has been extensively studied since the 19th century, after the work by Kelvin [14], in the special case of the motion of point vortices. Chorin pointed out that this approach can also be used for viscous flows. Its goal was to design efficient algorithms to compute turbulent flows [15]. Chorin proposed adding noise terms to the Hamiltonian motion equation for point vortices in order to take the viscosity into account. The deterministic motion equations of point vortices thus become *stochastic* equations. In a more rigorous approach, it can be shown that when the number of vortices tends to infinity, this stochastic system converges to a smooth solution of the (strong) Navier-Stokes equations [13,16]: the spatial distribution of point vortices approach the vorticity of a Navier-Stokes fluid. In this paper we show that this approach is also useful to obtain some theoretical insight into the dynamics of a few vortices, and to understand the influence of viscosity on the motion and interaction of vortices.

A particular solution of the weak Navier-Stokes equation is the Lamb vortex [17]. It is a point vortex that, under the effect of the viscosity, spreads in space. The Navier-Stokes equation reduces in this case to a heat equation, and the vorticity distribution is Gaussian. Clearly, from a stochastic point of view, the point vortex trajectory is one of a Brownian motion: the mean and standard deviations of the vortex position coincide with the moments of the Gaussian distribution. The vorticity is then directly related to the probability distribution of the point vortex position. Moreover, except at time $t=0$ (corresponding to the initial condition), the solution is also a strong solution of the Navier-Stokes equations. We will see that to study the interaction of a finite number (greater than one) of point vortices in a viscous medium, the links with the Navier-Stokes equations must be weaker; to make a proper discussion, it is necessary to introduce a stochastic formalism. This will be presented in detail in Sec. II.

The main objective of this paper is the study (part of these results have been presented in a letter [18]) of a system of *two* point vortices in a viscous medium, an obvious generalization of the Lamb problem. We will see that in such a case an exact solution can be found. In Sec. II a stochastic formalism is introduced, and a relation between the Navier-Stokes equation and a Fokker-Planck equation describing the probability distribution of point vortices is established. The specific case of two vortices is solved in Sec. III. The asymptotic properties of the solution at weak viscosity are

discussed in Sec. IV. The paper ends with a concluding section (Sec. VI), where in particular we discuss the physical significance of the solution.

II. DYNAMICS OF POINT VORTICES

Let us recall the basic properties of point vortices before focusing on their behavior in a viscous medium.

A. Euler dynamics of point vortices

We consider a vorticity field initially concentrated in a finite number of points \mathbf{x}_i , $i \in \{1, \dots, N\}$ in a two-dimensional domain D that we choose to be the plane, for the sake of simplicity ($D = \mathbb{R}^2$). Denoting $\delta(\mathbf{x})$ the Dirac measure at point \mathbf{x} , one writes the vorticity field

$$\omega(\mathbf{x}) = \sum_{i=1}^N \Gamma_i \delta(\mathbf{x} - \mathbf{x}_i) \quad \text{at } t=0. \quad (2.1)$$

Each term $\Gamma_i \delta(\mathbf{x} - \mathbf{x}_i)$ represents a point vortex (labeled by i) with circulation $\Gamma_i \neq 0$. The circulation can be defined by the identity $\Gamma_i = \int_C \mathbf{v}$, where C is any path surrounding the vortex i (and only this one). One can verify that the localization of the vorticity distribution is conserved in time,

$$\omega(\mathbf{x}, t) = \sum_{i=1}^N \Gamma_i \delta(\mathbf{x}_i(t) - \mathbf{x}), \quad (2.2)$$

with $\mathbf{x}_i(0) = \mathbf{x}_i$, which justifies the name of a field of point vortices $\omega(\mathbf{x}, t)$. Indeed, by inserting Eq. (2.2) into the momentum Euler equation (1.1), and using the divergence free constraint on the velocity field, one obtains

$$0 = \sum_{i=1}^N \Gamma_i \left\{ -\frac{d}{dt} \mathbf{x}_i(t) + \mathbf{v}(\mathbf{x}_i, t) \right\} \nabla_{\mathbf{x}} \delta(\mathbf{x}_i(t) - \mathbf{x}). \quad (2.3)$$

If we make the hypothesis that N vortices are never in contact at time t_f , by integration on balls of radii small enough (inferior to the smallest distance between two vortices) and centered at points $\mathbf{x}_i(t)$, one obtains that, for any time smaller than t_f ,

$$\frac{d}{dt} \mathbf{x}_i(t) = \mathbf{v}(\mathbf{x}_i, t). \quad (2.4)$$

Note that, for some particular initial conditions, collapse of several vortices can appear in a finite time [16,19,20]. Of course, Eqs. (2.3) and (2.4) are no longer valid after such a collapse. We see from Eq. (2.4) that the point vortices follow the field lines of the fluid, and that vorticity cannot be created or destroyed during the time evolution (in conformity with Helmholtz laws [21]).

Using the Biot-Savart law, one can retrieve the velocity field from the vorticity field,

$$\mathbf{v}(\mathbf{x}, t) = \frac{1}{2\pi} \int \frac{(\mathbf{x} - \mathbf{r}')^\perp}{|\mathbf{x} - \mathbf{r}'|^2} \omega(\mathbf{x}', t) d\mathbf{r}', \quad (2.5)$$

where \perp refers to a rotation of angle $+\pi/2$ in the counter-clockwise direction: $(x, y)^\perp = (-y, x)$. In the case of a set of point vortices, this last equality reduces to the simple expression

$$\mathbf{v}(x, t) = \sum_{i=1}^N \Gamma_i \mathbf{K}(\mathbf{x} - \mathbf{x}_i(t)), \quad (2.6)$$

where by definition $\mathbf{K}(\mathbf{x}) = (1/2\pi)\mathbf{x}^\perp/|\mathbf{x}|^2$ ($x \neq 0$) is the derivative of the Laplacian Green function (up to a rotation) in the plane (\mathbf{v} is zero at the infinity). Clearly this implies a divergence of the velocity field at point vortex positions $[|\mathbf{v}(\mathbf{x}_i, t)| = +\infty]$. A more rigorous derivation [16] shows that in fact the last equation is correct if we put $\mathbf{K}(0) = 0$. This condition simply means that a point vortex does not move under the effect of its self-rotation. Combination of identities (2.4) and (2.6) gives a set of differential equations which determines the evolution of the point vortex positions:

$$\frac{d}{dt} \mathbf{x}_i(t) = \sum_{j, j \neq i}^N \frac{\Gamma_j}{2\pi} \frac{(\mathbf{x}_j - \mathbf{x}_i)^\perp}{|\mathbf{x}_j - \mathbf{x}_i|^2}. \quad (2.7)$$

In the special case of only two vortices ($N=2$), one obtains

$$\frac{d}{dt} \mathbf{x}_i = \frac{\Gamma_j}{2\pi} \frac{(\mathbf{x}_j - \mathbf{x}_i)^\perp}{|\mathbf{x}_j - \mathbf{x}_i|^2}, \quad i \neq j. \quad (2.8)$$

Indices i and j can take values 1 and 2. A straightforward computation allows us to verify that the distance between the two vortices $r = |\mathbf{x}_1 - \mathbf{x}_2|$, and the mass center $\mathbf{M} = \Gamma_1 \mathbf{x}_1 + \Gamma_2 \mathbf{x}_2$, are first integrals of motion; their time derivatives are zero: $\dot{r} = 0$ and $\dot{\mathbf{M}} = 0$. If we do not consider the trivial case $\Gamma_1 \Gamma_2 r = 0$ and introduce $\Gamma = \Gamma_1 + \Gamma_2$, we obtain

$$\frac{d}{dt} \mathbf{x}_j = \frac{\Gamma_i}{2\pi \Gamma_j r^2} (\Gamma \mathbf{x}_j - \mathbf{M})^\perp, \quad (2.9)$$

which is the equation of a rotator (for $\Gamma \neq 0$), with rotation frequency $\Gamma \Gamma_i / 4\pi^2 \Gamma_j r^2$. As a consequence, either Γ is zero and the trajectories of vortices are two parallel straight lines, or it is different from zero and the trajectories are concentric circles of center \mathbf{M}/Γ .

It is interesting to note that a probabilistic interpretation of the point vortex dynamics of the Euler equation is possible. Let us introduce the probability transition density of a system of N vortices,

$$P(X, t) = \prod_{i=1}^N \delta(\mathbf{x}_i - \mathbf{x}(t; \mathbf{x}_{0i})), \quad (2.10)$$

where $X = \{\mathbf{x}_j\}$ is the point vortex configuration phase space, and $\mathbf{x}(t; \mathbf{x}_{0i})$ is a solution of the motion equation (2.7) with the initial condition $X_0 = \{\mathbf{x}_{0i}\}$. The meaning of Eq. (2.10) is simple: the probability that the vortex follows the trajectory given by Eq. (2.7) is 1. The equation of the probability density conservation in the vortex phase space X is

$$\frac{\partial}{\partial t} P + \nabla_X \cdot VP = 0, \quad (2.11)$$

where $V = \{\mathbf{v}(\mathbf{x}_i, t)\}$ is a vector whose components are the velocities of the point vortices, and ∇_X is the gradient operator in X space. Obviously solving Eq. (2.11) is equivalent to solving (for a system of point vortices) the Euler equation: in both cases one must solve the vortex motion equations (2.7). However, the interpretation of the results is different. In the Euler approach the knowledge of the vortex trajectories allows one to find the vorticity field at time t . In the probabilistic approach, one finds the probability that at time t the vortices are at a position X . As this probability is 1 if X is on the vortex trajectory, the two solutions are trivially equivalent. Note, however, that P depends on $2N+1$ variables (the vortex positions and time) and its evolution equation is linear, at variance to the original problem in which the vorticity is a function of only three variables (the two spatial coordinates and time) and satisfies a nonlinear equation. We see in Sec. II B that the relation between the two approaches in the case of a viscous fluid is complicated by the fact that the vorticity itself becomes a stochastic process.

B. Point vortices in a viscous medium

Let us now consider, in the spirit of relation (1.3), a set of N point vortices defining a vorticity field

$$\omega(x, t) = \sum_{i=1}^N \Gamma_i \delta(\mathbf{x} - \mathbf{x}_i(t)), \quad (2.12)$$

and let us assume that their velocities are no longer exactly equal to the fluid velocity generated by the other $N-1$ vortices at the positions they occupy [as in Eq. (2.4)], but are in addition perturbed by independent white noises $\{\mathbf{b}_1(t), \dots, \mathbf{b}_N(t)\}$:

$$\frac{d}{dt} \mathbf{x}_j(t) = \sum_{i=1, i \neq j}^N \Gamma_i \mathbf{K}(\mathbf{x}_j(t) - \mathbf{x}_i(t)) + \sqrt{2\nu} \mathbf{b}_j(t). \quad (2.13)$$

The white noises $\mathbf{b}_j(t)$ are random functions, invariant with respect to time translations; their mean value vanishes, $\langle \mathbf{b}_i \rangle(t) = 0$, and their cross correlation functions satisfy $\langle b_{i\alpha}(t) b_{j\beta}(t') \rangle = \delta_{ij} \delta_{\alpha\beta} \delta(t-t')$, where α stands for the spatial coordinate (x, y) .

The coefficient of the white noise terms $\sqrt{2\nu}$ is the same for all vortices, it is independent of i . Equations (2.12) and (2.13) show that the velocity of each vortex is the sum of two terms: the fluid velocity $\mathbf{v}(\mathbf{x}_i(t), t)$ at the vortex position, and a stochastic perturbation proportional to the fluid viscosity ν . To understand the origin of the viscous term we need to establish a link between this stochastic equation and the original Navier-Stokes equation. In order to establish this relation we start by computing the derivative of the vorticity [Eq. (2.12)],

$$\begin{aligned}
 \frac{\partial}{\partial t} \omega(\mathbf{x}, t) &= - \sum_{i=1}^N \Gamma_i \frac{d\mathbf{x}_i}{dt}(t) \cdot \nabla_{\mathbf{x}_i} \delta(\mathbf{x} - \mathbf{x}_i(t)) \\
 &= \sum_{i,j=1}^N \Gamma_i \Gamma_j \mathbf{K}(\mathbf{x}_j - \mathbf{x}_i) \cdot \nabla_{\mathbf{x}} \delta(\mathbf{x} - \mathbf{x}_i) \\
 &\quad + \sqrt{2\nu} \sum_{i=1}^N \Gamma_i \mathbf{b}_i \cdot \nabla_{\mathbf{x}} \delta(\mathbf{x} - \mathbf{x}_i) \\
 &= \sum_{j=1}^N \Gamma_j \mathbf{K}(\mathbf{x}_j - \mathbf{x}) \cdot \sum_{i=1}^N \Gamma_i \nabla_{\mathbf{x}} \delta(\mathbf{x} - \mathbf{x}_i) \\
 &\quad + \sqrt{2\nu} \nabla_{\mathbf{x}} \cdot \sum_{i=1}^N \Gamma_i \mathbf{b}_i \delta(\mathbf{x} - \mathbf{x}_i) \\
 &= -\mathbf{v}(\mathbf{x}, t) \cdot \nabla \omega(\mathbf{x}, t) + \sqrt{2\nu} \nabla_{\mathbf{x}} \cdot [\mathbf{b}(t) \omega(\mathbf{x}, t)],
 \end{aligned} \tag{2.14}$$

where, by definition, $\mathbf{b} = (\mathbf{b}_1, \dots, \mathbf{b}_N)$. This equation shows clearly that the vorticity of the system evolves according to a stochastic differential equation and the vorticity field at time t depends on the set of random noises $\{\mathbf{b}(s), 0 \leq s < t\}$.

Let us compute the stochastic mean of the last term in Eq. (2.14). The distribution of any white noise \mathbf{b}_i is Gaussian with mean zero. Dimensional analysis indicates that the variance σ^2 of a white noise is proportional to the inverse of a time. In fact, the white noise \mathbf{b}_i is defined from a Wiener process $\mathbf{W}(t)$, with $d\mathbf{W}(t)^2 = dt$, and it is such that $d\mathbf{W} = \mathbf{b}_i dt$. This last equality must be understood in the sense of the Ito stochastic calculus $\lim_{\Delta t \rightarrow 0} (\Delta \mathbf{W}(t)^2 - \Delta t) = 0$ [22]. It follows that the variance of each component of the white noise $b_{i\alpha}$ is formally given by $\sigma^2(t) = 1/(2dt)$ when $dt \rightarrow 0$.

We can now compute the stochastic mean of identity (2.14), using a Gaussian probability distribution for the white noise with variance σ^2 and zero mean. We note that $\mathbf{x} = (x_1, x_2)$, and $\langle A \rangle_{i\alpha}$, $\langle A \rangle_i$, and $\langle A \rangle$, the stochastic mean on random process $b_{i\alpha}$, \mathbf{b}_i , and \mathbf{b} , respectively. We obtain

$$\begin{aligned}
 &\langle \nabla_{\mathbf{x}} \cdot [\mathbf{b}_i \delta(\mathbf{x} - \mathbf{x}_i)] \rangle_i \\
 &= \int db_{i1} \int db_{i2} \frac{e^{-(b_{i1}^2 + b_{i2}^2)/2\sigma^2}}{2\pi\sigma^2} \\
 &\quad \times \left(b_{i1} \frac{\partial}{\partial x_1} \delta(\mathbf{x} - \mathbf{x}_i) + b_{i2} \frac{\partial}{\partial x_2} \delta(\mathbf{x} - \mathbf{x}_i) \right) \\
 &= -\sigma^2 \left\langle \int db_{i1} \frac{e^{-b_{i1}^2/2\sigma^2}}{\sqrt{2\pi\sigma^2}} \frac{\partial}{\partial b_{i1}} \frac{\partial}{\partial x_1} \delta(\mathbf{x} - \mathbf{x}_i) \right\rangle_{i2} \\
 &\quad - \sigma^2 \left\langle \int db_{i2} \frac{e^{-b_{i2}^2/2\sigma^2}}{\sqrt{2\pi\sigma^2}} \frac{\partial}{\partial b_{i2}} \frac{\partial}{\partial x_2} \delta(\mathbf{x} - \mathbf{x}_i) \right\rangle_{i1} \\
 &= -\sigma^2 dt \sqrt{2\nu} \sum_{\alpha=1}^2 \left\langle \frac{\partial}{\partial x_\alpha} \frac{\partial}{\partial x_\alpha} \delta(\mathbf{x} - \mathbf{x}_i) \right\rangle_i \\
 &= \left(\frac{\nu}{2} \right)^{1/2} \langle \nabla_{\mathbf{x}}^2 \delta(\mathbf{x} - \mathbf{x}_i) \rangle_i
 \end{aligned} \tag{2.15}$$

where we used the identity

$$\frac{\partial}{\partial b_{j\alpha}} \delta(\mathbf{x} - \mathbf{x}_j) = \sqrt{2\nu} dt \delta_{ij} \frac{\partial}{\partial x_\alpha} \delta(\mathbf{x} - \mathbf{x}_j),$$

which is a consequence of the Langevin equation (3.13). A rigorous derivation of these relations using functional integrals can be found in Ref. [23]. Combining Eqs. (2.14) and (2.15), one obtains the following result.

Proposition 1. A vorticity field of the form of Eq. (2.12), with the vortex trajectories satisfying the Langevin equation (2.13) is a stochastic solution of the following weak Navier-Stokes equation:

$$\left\langle \frac{\partial}{\partial t} \omega(\mathbf{x}, t) + \mathbf{v}(\mathbf{x}, t) \cdot \nabla \omega(\mathbf{x}, t) \right\rangle = \nu \langle \nabla^2 \omega(\mathbf{x}, t) \rangle. \tag{2.16}$$

Therefore, we established the link between the stochastic equation [Eq. (2.13)] describing the trajectories of the point vortices and the (weak form of the) Navier-Stokes equation (2.16). We conclude that the parameter ν , introduced in the Langevin equations, can effectively be identified with the viscosity. Instead of solving the stochastic dynamics by integration of the Langevin equations (2.13) and averaging over different realizations of the noise, one can introduce a Fokker-Planck equation [22] for the transition probability [a generalization of Eq. (2.11)],

$$\frac{\partial}{\partial t} P + \nabla_{\mathbf{x}} \cdot VP = \nu \Delta_{\mathbf{x}} P, \tag{2.17}$$

which gives a complete statistical description of the system evolution. Therefore, the problem is reduced to finding, from Eq. (2.17), the distribution probability of the point vortex positions. In Sec. III we give the explicit form of Eq. (2.17), and we compute the distribution P in the case of two vortices.

It is important to compare this result with the theorem of Marchioro and Pulvirenti [13], which is valid in the case of an infinite set of point vortices. Their statement is the following: Consider N vortices with circulation $\Gamma_i = \Gamma/N$ (Γ being fixed) satisfying, at $t=0$, $\lim_{N \rightarrow +\infty} \omega_N = \bar{\omega} \in L_1 \cap L_\infty(\mathbb{R}^2)$. The solution of the Navier-Stokes equation with initial data $\bar{\omega}$ is then, in the weak sense, equal to $\lim_{N \rightarrow +\infty} \omega_N$ at times $t \geq 0$.

The Marchioro-Pulvirenti theorem shows that a continuous vorticity field solution of the Navier-Stokes equation can be approached by using a very large number of interacting point vortices. Chorin was the first to use this technique to compute numerically the evolution of a vorticity field in a viscous medium [15].

When the number of vortices remains finite, we have a stochastic description of the dynamics (1). In particular the nonlinearity is in general such that $\langle \mathbf{v}(\mathbf{x}, t) \cdot \nabla \omega(\mathbf{x}, t) \rangle \neq \langle \mathbf{v}(\mathbf{x}, t) \rangle \cdot \nabla \langle \omega(\mathbf{x}, t) \rangle$, and no deterministic solution of the

Navier-Stokes equation is available in contrast to the case of a system of an infinite number of vortices. Nevertheless, obtaining a solution of such finite point vortex systems supplies a way to understand and illustrate the basic mechanisms involving the viscosity; this will be done in the simplest case in the next sections. Moreover, a solution for a small number of interacting vortices can describe some limiting cases of non-discrete vorticity fields on interesting time scales [24,25].

III. EXACT SOLUTION FOR THE INTERACTION OF TWO POINT VORTICES IN A VISCOUS FLUID

We consider two vortices with circulations Γ_1 and Γ_2 , initially separated by a distance r_0 , in a fluid of viscosity ν . Hereafter, we analyze this system in the simplest case, when both circulations are equal. Using these three parameters, the only dimensional parameters of the problem, one can form two characteristic times; the viscous time $t_\nu \sim r_0^2/\nu$ and the rotation time of the vortex pair, $t_\Gamma \sim r_0^2/\Gamma$ (we note that $\Gamma = \Gamma_1 + \Gamma_2$). The ratio of these two characteristic times gives the only nondimensional parameter of the problem, the Reynolds number $\text{Re} \sim \Gamma/\nu$. Because of the presence of a length scale (the initial distance r_0), in general one does not expect the evolution of the system to be self-similar. However, even in the case where a stochastic perturbation is present, the motion equations are invariant under the transformations $t \rightarrow \alpha^2 t$ and $\mathbf{x} \rightarrow \alpha \mathbf{x}$. This means that a scaling $\mathbf{x} \sim \sqrt{t}$ is compatible with both the deterministic and random parts of the vortex motion. In the inviscid case, another behavior compatible with the system's dimensions is possible: the trivial $\mathbf{x} \sim r_0$ scaling for which the distance between the two vortices remains constant. In the pure viscous case, a diffusive behavior is found with a normal scaling $\mathbf{x} \sim \sqrt{t}$, which also is the expected scaling for very long times. The problem is to find a solution matching these two different regimes.

A. Lamb vortex

In order to illustrate the stochastic approach to the Navier-Stokes dynamics, we start with the case of one isolated vortex. The vorticity is $\omega(\mathbf{x}, t) = \Gamma \delta(\mathbf{x} - \mathbf{x}_0(t))$, and the vortex motion equation simply reduces to a Brownian motion $\dot{\mathbf{x}}_0(t) = \sqrt{2\nu} \mathbf{b}(t)$. The transition probability $P = P(\mathbf{x}_0, t|0)$ then satisfies a Fokker-Planck equation, which is in this case a pure diffusion equation (without advection term)

$$\frac{\partial}{\partial t} P = \nu \Delta P, \quad P(\mathbf{x}_0, t|0) = \delta(\mathbf{x}_0), \quad (3.1)$$

assuming initially that the vortex is at the origin. The solution of the diffusion equation $P = P_L$ reads

$$P_L(\mathbf{x}_0, t) = \frac{1}{4\pi\nu t} \exp(-|\mathbf{x}_0|^2/4\nu t), \quad (3.2)$$

which is the usual Gaussian distribution. In addition, the vorticity can be obtained using,

$$\langle \omega \rangle(\mathbf{x}, t) = \Gamma \int_{\Omega} P_L(\mathbf{x}_0, t) \delta(\mathbf{x} - \mathbf{x}_0) d\mathbf{x}_0 = \Gamma P_L(\mathbf{x}, t), \quad (3.3)$$

which gives the well-known Lamb vortex [17]. In this case the role of the viscosity is simply related to the diffusion of the initially concentrated vorticity, and the vortex size grows as \sqrt{t} . We will see that, for the two vortices, basic mechanisms induced by the viscosity appear.

B. Probability density of two corotating point vortices

We now investigate the evolution of a system of two point vortices. We look for a solution of Eqs. (2.12) and (2.13) in the special case $N=2$. In the light of the results for the case $N=1$, we can interpret Eqs. (2.12) and (2.13) as describing the interaction of two Lamb vortices. Therefore, the vorticity field evolves according to a stochastic process depending on the paths $\{\mathbf{x}_1(t), \mathbf{x}_2(t)\}$. In order to describe this system one must determine the probability distribution of the vortex positions $P(\mathbf{x}_1, \mathbf{x}_2, t)$, and then solve the Fokker-Planck equation it satisfies. As the vortex trajectories are stochastic, the transition probability in this framework becomes the basic quantity from which one may calculate other physical quantities as, for instance, the mean vorticity distribution $\langle \omega \rangle$ [see Eq. (3.5)], or the characteristic merging time.

When $\Gamma_1 = \Gamma_2$, the noise terms in the Langevin equations for $\mathbf{r} = \mathbf{x}_1 - \mathbf{x}_2$ and $\mathbf{M} = (\Gamma/2)(\mathbf{x}_1 + \mathbf{x}_2)$ are independent because

$$\left\langle \frac{\Gamma}{2} (\mathbf{b}_1 - \mathbf{b}_2)(\mathbf{b}_1 + \mathbf{b}_2) \right\rangle(t) = \frac{\Gamma}{2} [\langle \mathbf{b}_1^2 \rangle(t) - \langle \mathbf{b}_2^2 \rangle(t)] = 0.$$

Hence the two vortex transition probability $P(\mathbf{x}_1, \mathbf{x}_2, t)$ turns out to be the product of the probability distributions of the center of mass $P_{\mathbf{M}}$ and of the vortex distance $P_{\mathbf{r}}$: $P(\mathbf{x}_1, \mathbf{x}_2, t) = P_{\mathbf{M}}(\mathbf{M}, t) P_{\mathbf{r}}(\mathbf{r}, t)$. The knowledge of these probabilities allows the computation of the observed vorticity evolution by direct integration:

$$\begin{aligned} \langle \omega \rangle(\mathbf{x}, t) &= \int P(\mathbf{x}_1, \mathbf{x}_2, t) \omega(\mathbf{x}, t; \mathbf{x}_1, \mathbf{x}_2) d\mathbf{x}_1 d\mathbf{x}_2 \quad (3.4) \\ &= (\Gamma/2) \int [P(\mathbf{x}, \mathbf{y}, t) + P(\mathbf{y}, \mathbf{x}, t)] d\mathbf{y}. \end{aligned} \quad (3.5)$$

Using Eq. (2.13) we immediately find that the center of mass \mathbf{M} follows a Brownian motion,

$$\frac{d}{dt} \mathbf{M}(t) = \Gamma \sqrt{\nu} \mathbf{B}(t), \quad (3.6)$$

where $\mathbf{B} = [\mathbf{b}_1(t) + \mathbf{b}_2(t)]/2^{1/2}$ is a unit variance white noise. Therefore, $P_{\mathbf{M}}$ is a Gaussian probability distribution:

$$P_{\mathbf{M}} = \frac{1}{2\pi\Gamma^2\nu t} \exp\left[-\frac{M^2}{2\nu\Gamma^2 t}\right]. \quad (3.7)$$

Moreover, the distance \mathbf{r} satisfies the Langevin equation

$$\frac{d}{dt}\mathbf{r}(t) = \Gamma\mathbf{K}(\mathbf{r}) + 2\sqrt{\nu}\mathbf{b}(t), \quad (3.8)$$

where $\mathbf{b}(t) = [\mathbf{b}_1(t) - \mathbf{b}_2(t)]/2^{1/2}$ is still a white noise. The Fokker-Planck equation associated with Eq. (3.8) is [26]

$$\frac{\partial}{\partial t}P_r(\mathbf{r}, t) = -\Gamma\nabla \cdot [P_r(\mathbf{r}, t)\mathbf{K}(\mathbf{r})] + 2\nu\Delta P_r(\mathbf{r}, t). \quad (3.9)$$

We introduce the polar coordinates $\mathbf{r} = (r, \theta)$, then the velocity kernel is written $\mathbf{K}(\mathbf{r}) = \hat{\mathbf{e}}_\theta/2\pi r$. We also introduce the following units: r_0 , the initial vortex distance, for the length; and $2\pi r_0^2/\Gamma$ for the time. The Reynolds number is thus $\text{Re} = \Gamma/4\pi\nu$. In addition, we suppose $r_0 \neq 0$; otherwise we would just obtain a Lamb vortex of circulation Γ . In the following (r, t, ν) will stand for the nondimensional quantities where the new ν is $1/\text{Re}$. Using these notations we rewrite the last equation in the form

$$\frac{\partial}{\partial t}P_r(r, \theta, t) = -\frac{1}{r^2}\frac{\partial}{\partial\theta}P_r(r, \theta, t) + \nu\Delta P_r(r, \theta, t), \quad (3.10)$$

where Δ is the Laplacian in polar coordinates:

$$\Delta = \frac{\partial^2}{\partial r^2} + \frac{1}{r}\frac{\partial}{\partial r} + \frac{1}{r^2}\frac{\partial^2}{\partial\theta^2}. \quad (3.11)$$

It is remarkable that an equation similar to Eq. (3.10) appeared, in a completely different context, as the equation for the vorticity of a spiraling sheet [see Eq. (30) of Lundgren's paper on strained spiral vortices and turbulence [8]]. However, although the vortex sheet equation with viscous corrections of Lundgren and the Fokker-Planck equation for the distance between two point vortices are formally similar, they differ by the initial condition and the normalization constraint that the transition probability must satisfy and that do not apply to the vorticity. This analogy will prove useful in discussing the intermediate time asymptotics of the merging process (see Sec. IV below).

C. Computation of the distance probability distribution

We now compute the solution of Eq. (3.10) with initial conditions, given in polar coordinates, $P_r(r, \theta, 0) = \delta(r-1, \theta - \theta_0)$, which means that the initial distance between the two vortices is 1 and the initial inclination of the vortex pair is θ_0 . The Fokker-Planck equation being invariant by rotation, one can choose $\theta_0 = 0$ without loss of generality. The initial condition can then be written

$$P(r, \theta, 0) = \delta(r-1, \theta). \quad (3.12)$$

Let us look for functions with separate variables belonging to the kernel of the Fokker-Planck operator, such that $P = G(r, t)f(\theta)$. By inserting functions G and f and multiplying Eq. (3.10) by $r^2/(Gf)$, we obtain an identity where f and G are separated:

$$\frac{1}{G}\left(\frac{r^2}{\nu}\frac{\partial}{\partial t} - r^2\frac{\partial^2}{\partial r^2} - r\frac{\partial}{\partial r}\right)G = \frac{1}{f}\left(-\frac{1}{\nu}\frac{\partial}{\partial\theta} + \frac{\partial}{\partial\theta^2}\right)f. \quad (3.13)$$

The right hand side is independent of θ , and the left hand side is independent of r, t . This implies that the two terms are equal to a constant, say λ_1 , which gives the two equations

$$\frac{\partial}{\partial\theta^2}f - \frac{1}{\nu}\frac{\partial}{\partial\theta}f - \lambda_1 f = 0, \quad (3.14)$$

$$\frac{\partial^2}{\partial r^2}G + \frac{1}{r}\frac{\partial}{\partial r}G + \frac{\lambda_1}{r^2}G = \frac{1}{\nu\partial}\frac{\partial}{\partial t}G.$$

It is even possible to get a separate variables solution for G . Inserting $G(r, t) = g(r)h(t)$ into the above equation, we obtain

$$\frac{1}{g(r)}\left(\frac{\partial^2}{\partial r^2} + \frac{1}{r}\frac{\partial}{\partial r} + \frac{\lambda_1}{r^2}\right)g(r) = \frac{1}{\nu h(t)}\frac{\partial}{\partial t}h(t) = \lambda_2, \quad (3.15)$$

where λ_2 is another undetermined constant. From the second equality one obtains $h = e^{\lambda_2\nu t}$. The linearity of Eq. (3.10) implies that the more general solution that we can deduce is

$$P(r, \theta, t) = \int d\lambda_1 d\lambda_2 a(\lambda_1, \lambda_2) e^{\lambda_2\nu t} f_{\lambda_1}(\theta) g_{\lambda_1, \lambda_2}(r), \quad (3.16)$$

where we explicitly write the parameter dependence of g and f , and the complex function $a: \mathbb{C} \times \mathbb{C} \rightarrow \mathbb{C}$ is to be determined by imposing the initial condition [Eq. (3.12)]. Note that Eq. (3.16) may be a generator of the set of solutions of class \mathbb{C}^2 or of any other functional space. In fact, by determining now the Green function of the Fokker-Planck equation, we are showing that this is (fortunately) the case. By definition the Green function satisfies the initial condition [Eq. (3.12)]. In order to match Eq. (3.16) with Eq. (3.12) at time $t=0$, we need to reformulate this last equation. By denoting $k = |\mathbf{k}|$ and making use of the equality

$$\exp(iz \cos(\theta)) = \sum_{l=-\infty}^{+\infty} i^l J_l(z) \exp(il\alpha), \quad (3.17)$$

where $z = k|\mathbf{r} - \mathbf{r}_0|$ and α is the angle $(\mathbf{k}, \mathbf{r} - \mathbf{r}_0)$, we obtain

$$\begin{aligned} \delta(\mathbf{r} - \mathbf{r}_0) &= \frac{1}{4\pi^2} \int d\mathbf{k} \exp(i\mathbf{k} \cdot [\mathbf{r} - \mathbf{r}_0]) \\ &= \frac{1}{4\pi^2} \int_0^{+\infty} dk \int_0^{2\pi} k \exp(ik|\mathbf{r} - \mathbf{r}_0| \cos \alpha) \\ &= \frac{1}{2\pi} \int_0^{+\infty} dk k J_0(k|\mathbf{r} - \mathbf{r}_0|). \end{aligned} \quad (3.18)$$

The Bessel function J_0 can be rewritten in a form where the polar coordinate variables r and θ are separated. By using a Bessel function development [27], we can finally write the initial condition as

$$\delta(\mathbf{r}-\mathbf{r}_0)=\frac{1}{2\pi}\int_0^{+\infty}dkk\left[J_0(kr_0)J_0(kr)+2\sum_{p=1}^{+\infty}J_p(kr_0)J_p(kr)\cos(p\theta)\right]. \quad (3.19)$$

The form of this last expression clearly indicates what to do now. Indeed, Bessel functions J_p are a subset of the set of solutions $\{g_{\lambda_1,\lambda_2},(\lambda_1,\lambda_2)\in\mathbb{C}\times\mathbb{C}\}$. With $\lambda_1<0,\lambda_2<0$ and by introducing $R=r\sqrt{|\lambda_2|}$, from Eq. (3.15) we obtain a new equation for $g=g_{\lambda_1,\lambda_2}$:

$$\frac{\partial^2}{\partial R^2}g(R)+\frac{1}{R}\frac{\partial}{\partial R}g(R)+\left[1-\frac{|\lambda_1|}{R^2}\right]g(R)=0. \quad (3.20)$$

Its general solution is a linear combination of the first kind Bessel functions with order parameter $\sqrt{|\lambda_1|}$,

$$g(r)=C_1J_{\sqrt{|\lambda_1|}}(r\sqrt{|\lambda_2|})+C_2N_{\sqrt{|\lambda_1|}}(r\sqrt{|\lambda_2|}), \quad (3.21)$$

where C_1 and C_2 are the integration constants. So we have to choose between two kinds of solutions formally equal to Eq. (3.19) at $t=0$: either we may decide to have an integer parameter in the order p of the Bessel $J_p(\theta)$ ($p=\sqrt{|\lambda_1|}$), or we may decide to solve for cosine functions $\cos(p\theta)$ [with $p=(1\pm\sqrt{1+4|\lambda_1|})/2\in\mathbb{N}$]. One can verify that in the first case we obtain solutions satisfying the initial condition but that are not derivable along $\theta=0$. The second case leads to a solution of the form

$$P(r,\theta,t)=\frac{1}{2\pi}\sum_{p\in\mathbb{Z}}e^{ip\theta}\times\int_0^{+\infty}\lambda_2d\lambda_2e^{-\lambda_2^2\nu t}J_{\mu_p}(\lambda_2r)J_{\mu_p}(\lambda_2r_0), \quad (3.22)$$

where $\{\mu_p\in\mathbb{C}:\mu_p^2=ip/\nu+p^2,\Re\mu_p\leq 0,p\in\mathbb{N}\}$ is the set of constants λ_1 we choose (\Re stands for the real part). In dimensional variables we have the expression $\mu_p^2=i\Gamma p/(4\pi\nu)+p^2$, and in the limit $\Gamma\rightarrow 0$, we at $t=0$ we exactly obtain expression (3.19). We will verify that in the case $\Gamma\neq 0$, the initial condition is also verified. Expression (3.22) can be integrated using the formula [27]

$$\int_0^{+\infty}e^{-\rho^2x^2}J_\gamma(\alpha x)J_\gamma(\beta x)x dx=\frac{1}{2\rho^2}\exp\left(-\frac{\alpha^2+\beta^2}{4\rho^2}\right)I_\gamma\left(\frac{\alpha\beta}{2\rho^2}\right), \quad (3.23)$$

$\Re\gamma>-1,|\arg\rho|<\pi/4,\alpha>0,\beta>0,$

where $\alpha=r$, $\beta=r_0=1$, $\gamma=\mu_p$, $\rho^2=\nu t$, and $x=\lambda_2$. I_γ are modified Bessel functions. The general solution is finally written as

$$P_r(r,\theta,t)=G(r,t)\left[1+2\Re\sum_{p=1}^{+\infty}I_0^{-1}\left(\frac{r}{2\nu t}\right)I_{\mu_p}\left(\frac{r}{2\nu t}\right)e^{ip\theta}\right], \quad (3.24)$$

where the radial part of the distribution is

$$G(r,t)=\frac{1}{4\pi\nu t}\exp\left(-\frac{r^2+1}{4\nu t}\right)I_0\left(\frac{r}{2\nu t}\right). \quad (3.25)$$

We now check that the solution found [Eq. (3.24)] indeed satisfies the initial condition. An important property of the Bessel functions $I_\mu(x)$ is that they are all equivalent in the limit $x\rightarrow+\infty$, independently of the order μ . Formally, if we take as their common limit I_0 , we can write

$$P_r(r,\theta,t)\sim G(r,t)\delta(\theta), \quad (t\rightarrow 0), \quad (3.26)$$

which gives the expected limit [Eq. (3.12)] as $t\rightarrow 0$.

In conclusion, the vorticity field associated with Eq. (3.24) and the Gaussian distribution P_M of Eq. (3.2) is the exact solution of the stochastic two-dimensional Navier-Stokes equation. The proof that Eq. (3.24) is effectively a normalized positive probability distribution is deferred to Sec. V.

Equation (3.24) is the Green function of the Fokker-Planck equation (3.10), and gives the temporal evolution of the distance between the two initial point vortices. Of course, the limiting case $\text{Re}=1/\nu=0$, that is to say when the two vortex system is dominated by viscosity, gives $\mu_p=p$, and the solution becomes $P_L(\mathbf{r}-\mathbf{r}_0,t)$. The evolution of the distance reduces therefore to a Brownian motion, as one could also derive directly using the Langevin equation without the velocity term.

The probability $G(r,t)$ is the axisymmetric part of P_r , and can also be obtained as the solution of the heat equation, with the initial condition a distribution of the vorticity along a ring. This characterizes the diffusion of the radial distance. It is worth noting that this axisymmetric part becomes asymptotically dominant in the limit of long times $t\rightarrow+\infty$ [$I_\mu(0)=\delta_{0,\mu}$, the Kronecker δ], demonstrating that the final state of the system is isotropic. Therefore, solution (3.24) describes the change in the topology of the flow: the initial state of two localized vortices evolve to an axisymmetric structure.

IV. ASYMPTOTIC ANALYSIS OF THE PROBABILITY DISTRIBUTION

General formula (3.24) is quite abstract and, because of the Bessel functions of complex order, its numerical evaluation is not easy. However, some useful information can be obtained in the limit of small viscosity using asymptotic expansions. The difference between Euler ($\nu=0$) and Navier-Stokes ($\nu=0^+$) equations can be studied in detail from expression (3.10). When ν is zero, the solution of Eq. (3.8), in polar coordinates, is

$$r=1, \quad \frac{d}{dt}\theta=1, \quad (4.1)$$

where $(1, \theta_0)$ is the initial distance, and corresponds to a rotation of period $T = 2\pi$. A probability distribution associated with this deterministic motion is

$$P_r(r, \theta, t) = \delta(r - 1, \theta - t - \theta_0). \quad (4.2)$$

This is of course a solution to Eq. (3.10), with $\nu = 0$. An important question arises about the influence of the viscosity. First, we note that the argument of the angular Dirac function may be rewritten in the form $\theta - t f(r) - \theta_0$, where f is an arbitrary function satisfying $f(1) = 1$. Second, for any arbitrary small viscosity (in fact, $\nu \rightarrow 0^+$) under the effect of diffusion, the δ functions in Eq. (4.2) will spread out. Therefore, the actual distance (in the probabilistic sense) between the vortices will be slightly different from $r_0 = 1$, which raises the problem of the choice of f . This is precisely the role of the viscosity, which will select a particular form of f , compatible with the Navier-Stokes equation, as we show below.

A. Weak viscosity development

After a factorization of the radial part, an asymptotic expansion in powers of νt of Eq. (3.24) can be obtained:

$$P(r, \theta, t) = G(r, t) \sum_{n=0}^{+\infty} \nu^n t^n P_n(r, \theta, t; \nu), \quad (4.3)$$

with

$$\int_{\Omega} P_0 = 1 \quad (4.4)$$

and

$$\int_{\Omega} P_n = 0, \quad n \geq 1. \quad (4.5)$$

In fact, in this section we compute the first two terms of the series. By construction, the asymptotic expansion [Eq. (4.3)] is done in such a way to obtain a better understanding of the nonisotropic part of the probability distribution, which is in fact the mathematically complex part of the expression.

We start by presenting the order zero term computation P_0 , and verify that this is the theta elliptic function $\Theta(n=0)$. We make use of a Bessel function expansion [27]

$$I_{\mu}(x) = \frac{e^x}{\sqrt{2\pi x}} \sum_{q=0}^{+\infty} (-1)^q \Gamma_{q, \mu}(x), \quad (4.6)$$

where

$$\begin{aligned} \Gamma_0(x) &= 1, \quad \Gamma_{q, \mu}(x) \\ &= \frac{(4\mu^2 - 1) \cdots (4\mu^2 - [2q - 1]^2)}{q!(8x)^q}, \\ & \quad q \in \mathbb{N}^*. \end{aligned} \quad (4.7)$$

This development is valid when the argument of x is between $-\pi/2$ and $+\pi/2$ and in particular when x is positive, for x large (going to infinity). However, one should note that such an expansion is divergent in the usual sense of the term. The equality written in Eq. (4.6) is to be understood in the formal series sense. In fact, the coefficient series is itself divergent, because when $q \rightarrow +\infty$, the main contribution to $\Gamma_{q, \mu}$ is

$$\Gamma_{q, \mu} \sim f(\mu) \frac{\prod_{i=1}^q (2i-1)^2}{q!(8x)^q} \sim 4f(\mu) \frac{q!}{(8x)^q}, \quad (4.8)$$

where $f(\mu)$ does not depend on q . It follows that $\lim_{q \rightarrow +\infty} \Gamma_{q, \mu} = f(\mu) \times \infty$, so that the divergence is very strong. The convergence is, as stated by Poincaré [28], in the astronomer's sense and not in the geometrician's. Actually, this expansion converges, when x is not too small (for a fixed μ value), exponentially close to $I_{\mu}(x)$, with the condition that the summation is stopped at a well chosen index $q(x, \mu)$. Indeed, the first terms of the series $\Gamma_{q, \mu}$ decreases to 0 (in absolute value) because of the denominator x^q . This is called a "quasiummation to the smaller term." In practice, a convenient choice of index is the one where the summation $\Gamma_{q, \mu}$ ceases to be a decreasing function of q , which numerically gives results of the precision machine order. So it would be more judicious to write

$$q_0 = \min\{q \in \mathbb{N}, |\Gamma_{q, \mu}(x)/\Gamma_{q-1, \mu}(x)| \leq 1\}, \quad (4.9)$$

$$I_{\mu}(x) = \frac{e^x}{\sqrt{2\pi x}} \sum_{q=0}^{q_0} (-1)^q \Gamma_{q, \mu}(x). \quad (4.10)$$

A rigorous theory about asymptotic divergent series was developed quite recently by Ramis [29]. The main theorem states that a formal series solution of a differential equation (with analytic coefficients, which is our case) is the (Gevrey) asymptotics of an exact solution of the differential equation. Identity (4.10) is a particular case of this theorem.

In the case we are interested in, we have $x = \bar{x} = r/2\nu t$ and $\mu = \mu_p$. We now focus on finding the dominant terms in the $\Gamma_{q, \mu}(x)$ of sum (6.6), in the limit $\nu \rightarrow 0$. We note that it is not correct to keep only the term with the lowest order in ν , because in the highest order Bessel functions $I_{\mu_p}(p \rightarrow +\infty)$ these are no longer dominant. As a consequence, we have to keep the polynomial contributions with the highest degree in p . In fact, in the identity

$$q! \Gamma_{q, \mu}(\bar{x}) = \frac{1}{r^q} \prod_{j=1}^q \left[p^2 \nu t + i p t - \left(j - \frac{1}{2} \right)^2 \nu t \right], \quad (4.11)$$

the dominant term when ν is small is $i p t$, except when the integer p is large. In this last case, $p^2 \nu t$ is dominant. The third term $(j - \frac{1}{2})^2 \nu t$ is, in a first approximation, negligible in all cases under the condition that the quasiummation satisfies $q_0^2 \nu \leq 1$. The larger is $x = \bar{x}$, the better this is verified. Finally, we can write

$$\Gamma_{q,\mu}(\bar{x}) = \frac{1}{q!} \left(\frac{p^2 vt + ipt}{r} \right)^q. \quad (4.12)$$

By introducing this approximation into Eq. (4.6) we obtain a rapidly converging series [with a general term $(-1)^q \Gamma_{q,\mu}$]. We can then extend the summation to infinity, which gives

$$\begin{aligned} I_0^{-1}(\bar{x}) I_{\mu_p}(\bar{x}) &= \sum_{q=0}^{+\infty} \frac{1}{q!} \left(-\frac{p^2 vt + ipt}{r} \right)^q \\ &= \exp \left(-\frac{p^2 vt + ipt}{r} \right). \end{aligned} \quad (4.13)$$

Now we just have to sum the terms $I_0^{-1} I_{\mu_p} \exp(ip\theta)$. By using the canonical transformation ($\epsilon > 0$)

$$S(\epsilon, \phi) = \sum_{m \in \mathbb{Z}} e^{-\epsilon n^2 + 2i\pi n \phi} = \left(\frac{\pi}{\epsilon} \right)^{1/2} \sum_{n \in \mathbb{Z}} e^{-(\pi^2/\epsilon)(n-\phi)^2}, \quad (4.14)$$

with $\epsilon = vt/r$ and $2\pi\phi = -t/r + \theta$, we finally obtain an approximation of Eq. (3.24),

$$P_r(r, \theta, t) \sim G(r, t) \Theta(r, \theta, t), \quad \nu \rightarrow 0, \quad (4.15)$$

where the asymmetric part of the right-hand term of Eq. (4.15) is the theta function [27],

$$P_0 = \Theta(r, \theta, t) = \left(\frac{\pi r}{2vt} \right)^{1/2} \sum_{p=-\infty}^{+\infty} e^{-(\pi^2 r/vt)(p - (1/2\pi)[\theta - (t/r)])^2}. \quad (4.16)$$

The function Θ is a solution of the one-dimensional heat equation on the circle. In the present context, it describes the development of a spiral structure we will call S , triggered by the interaction of the vortices. We note that the spiral stretching (dispersion of the angular part of the probability distribution) increases as t while the diffusion goes as $t^{1/2}$, so that the development of the spiral structure is faster than the radial diffusion.

A noteworthy point in the asymptotic estimation [Eq. (4.16)] is that we still obtain a probability distribution. Indeed, an easy computation allows to verify Eq. (4.4), and positivity is obvious. This calculation is interesting because of the role played by the large order Bessel functions ($p \rightarrow +\infty$): they determine the ‘‘nonzero viscosity’’ properties of the solution. They allow a quantification of the thickening of the spiral S at small times. The other Bessel functions give geometrical properties of the solution, the $\nu=0^+$ limit [see Eq. (4.24)].

In the same way as the ν dependence of the function Θ is associated with the spiral thickness where the distribution is concentrated, the order n corrections $P_n(\nu)$ do not modify the geometrical properties of the distribution (spiral structure), and the ν dependence remains related to the effect of thickening.

This can be verified by computing the order one correction P_1 ($n=1$). In Eq. (4.6), the terms of higher order are (i) the first order term in $(4\mu^2/8\bar{x})^q/q!$, and (ii)

$(-1/4\mu^2) \sum_{i=0}^{q-1} (2i-1)^2$ times the zero order term $(4\mu^2/8\bar{x})^q/q!$. As before, noting that $\mu^2 = o(p^2, p/\nu)$, we keep the dominant term at ν small and p large, and neglect the divergent part in q (which will allow us to compute the infinite sum). Therefore, we can write

$$\left(\frac{4\mu^2}{8\bar{x}} \right)^q = \left(\frac{vp^2}{r} + i \frac{pt}{r} \right)^q, \quad (4.17)$$

$$\frac{1}{4\mu^2} = -\frac{i\nu}{4p} \frac{1}{(1-i\nu p)} = -\frac{i\nu}{4p} + o(\nu), \quad (4.18)$$

$$\sum_{i=0}^{q-1} (2i-1)^2 = \frac{1}{3} q(4q^2-1). \quad (4.19)$$

Approximation (4.18) breaks down when p is of order equal or larger than ν^{-1} , but in this case we obtain a term of order ν^2 which is negligible. Hence we obtain

$$q! \Gamma_{q,\mu} = \left(\frac{ipt + vp^2}{r} \right)^q \left[1 - i\nu \frac{q}{12p} + i\nu \frac{q^3}{3p} + o(\nu) \right]. \quad (4.20)$$

To complete the estimation of $I_\mu(\bar{x})$, we make use of the identities

$$\sum_{q=0}^{+\infty} q \frac{x^q}{q!} = x e^x, \quad \sum_{q=0}^{+\infty} q^3 \frac{x^q}{q!} = (x^3 + 3x^2 + x) e^x,$$

to obtain

$$\begin{aligned} I_{\mu_p}(\bar{x}) &= \frac{\exp(\bar{x})}{\sqrt{2\pi\bar{x}}} \exp \left(\frac{-ipt - vp^2}{r} \right) \\ &\times \left\{ 1 + \nu \left[\frac{t}{4r} - ip \frac{t^2}{r^2} - p^2 \frac{t^3}{3r^3} \right] + o(\nu) \right\}. \end{aligned} \quad (4.21)$$

We just have to insert Eq. (4.21) into the general expression Eq. (3.24) to obtain P_1 . Collecting all the terms, we finally obtain

$$\begin{aligned} P_0(r, \theta, t) + \nu P_1(r, \theta, t) \\ = \Theta(r, \theta, t) - 2\nu \frac{t^2}{r^2} \sum_{p=1}^{+\infty} \left[p e^{-p^2 vt/r} \sin(p[\theta - t/r]) \right. \\ \left. + \frac{t}{3r} p^2 e^{-p^2 vt/r} \cos(p[\theta - t/r]) \right]. \end{aligned} \quad (4.22)$$

Note that the correction does not diverge in the limit $t/r \rightarrow +\infty$ because of the exponentials in sums (4.22). It is straightforward to see that the mean of the correction is zero, as stated in Eq. (4.5). It is also interesting to see that the correction P_1 is still localized on the spiral S . Indeed, in the limit $\nu \rightarrow 0$, the correction becomes a sum of derivatives of the delta function $\delta(S)$:

$$P_1(r, \theta, t) = \frac{2t^2}{r^2} \delta'(\theta - t/r) + \frac{2t^3}{3r^3} \delta''(\theta - t/r). \quad (4.23)$$

Therefore, we have obtained the first terms of a polynomial development in powers of ν of a multipolar nature. The coefficients of this development are functions of space and time whose support is geometrically concentrated on the spiral, in the limit of time scales small compared with the viscous time. The spreading of the probability in the angular direction has a characteristic scale $r \sim t$ of the ballistic type. The spreading process is then dominated by kinematic effects, related to the deterministic rotation of the vortex pair.

As mentioned above (Sec. III B) Lundgren [8] analyzed an equation similar to Eq. (3.10) in his study of stretched vortex spirals. He found an intermediate asymptotic regime, between the “ballistic” and the “viscous” regimes, characterized by a time scale $\tau_L \sim 1/\nu^{1/3}$ (or $\Gamma \tau_L / r_0^2 \sim (\Gamma/\nu)^{1/3}$ in dimensional variables). This intermediate regime appears for times in the range $1 \ll \nu^{1/3} t \ll \nu^{-1/6}$ (in a first approximation). The main consequence of the existence of this regime is that the harmonics of the angular probability distribution decay faster than the radial distribution (the axisymmetric part of the probability distribution diffuse with a characteristic viscous scale).

B. Description of the merging process

In the limit $\nu = 0^+$, Eq. (4.16) gives the angular probability distribution

$$\Theta(r, \theta, t) = \delta(\theta - t/r), \quad (4.24)$$

which corresponds to a concentration of the probability on a spiral (in the original units) $S: \theta \rightarrow \theta(r) = \Gamma t / 2\pi r_0 r$, centered at $r = 0$ and spreading in time. The emergence of this spiral structure (decreasing as $1/r$) is the result of a selection by the viscosity [selection of $f(x) = 1/x$] coupled with the rotation effect ($\Gamma \neq 0$). Therefore, the viscosity is not only important for its effect on diffusion and topology change, but also in selecting a particular spiral structure. The particular form of f , at least for small viscosity, may be related to the conservation of the angular velocity $v_\theta = r\dot{\theta} = \Gamma / 2\pi r_0$. Expression (4.16) adds a “Gaussian thickness” to the spiral structure. Of course, if we set $\nu = 0$ for the radial and nonradial parts of $P_{\mathbf{r}}$, we obtain the expected limit: the evolution of the distance between two point vortices [Eq. (4.2)].

In addition the probability distribution on the spiral structure follows the law $G(r, t)$ and has a sharp maximum at $r_p(t)$, the solution of the implicit equation (returning to dimensionless quantities)

$$r_p = \frac{I_1\left(\frac{r_p}{2\nu t}\right)}{I_0\left(\frac{r_p}{2\nu t}\right)} \leq 1. \quad (4.25)$$

For $t = 0$, r_p is equal to 1 and decreases to zero as time grows. In Fig. 1 we plot $r_p = r_p(t)$. The important point is

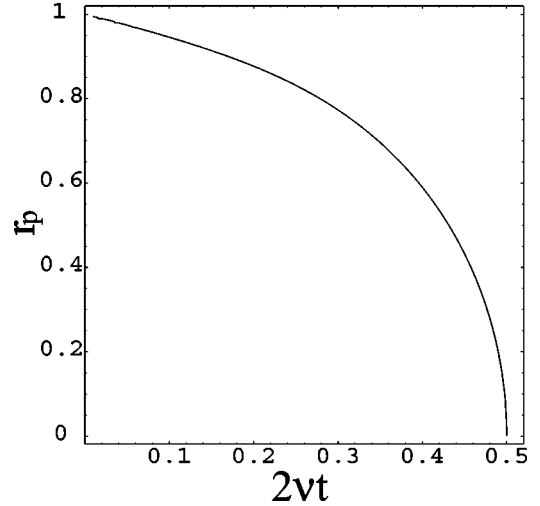


FIG. 1. Evolution of the distance between the two probability maxima $r_p(t)$.

that the distance between the vortices goes to zero in a *finite* time. For small times we have

$$r_p \approx 1 - \nu t / 2, \quad (4.26)$$

the almost constant distance behavior expected for small viscosity. For times approaching $t \approx 1/4\nu$ the distance collapses following the power law

$$r_p \approx \sqrt{2}(1 - 4\nu t)^{1/2}, \quad (4.27)$$

which satisfies the scaling $\mathbf{x} \sim \sqrt{t}$ common to the deterministic and diffusive regimes. We see that Eq. (4.25) satisfies the requirement stated above, that the solution must match the deterministic scaling with the viscous one.

In order to obtain a representation of the dynamics of the system, we combine the results on the behavior of the axisymmetric part of the probability distribution with the angular part. The two asymptotic regimes, where r_p are given by Eqs. (4.26) and (4.27), respectively correspond to two spiral forms (following the maximum of the distance probability distribution):

$$r \approx \frac{1}{1 + \frac{\nu\theta}{2}}, \quad (4.28)$$

which is valid for $r \approx 1$; and

$$r \approx 2\nu\theta - \sqrt{(2\nu\theta)^2 + 1}, \quad (4.29)$$

which is valid for $r \approx 0$. These expressions show clearly the structure of the vortex spiral trajectories $r = r(\theta)$ as a function of the Reynolds number $1/\nu$.

Let us discuss a specific case. The actual distribution is obtained from the product of the spiral S and the radial structure. The thickness of the radial probability maximum is given by $(\nu t)^{1/2}$, and is narrow in the limit of small viscosity. Depending on the position of this peak on the spiral, different behaviors may be obtained, as can be seen by a detailed

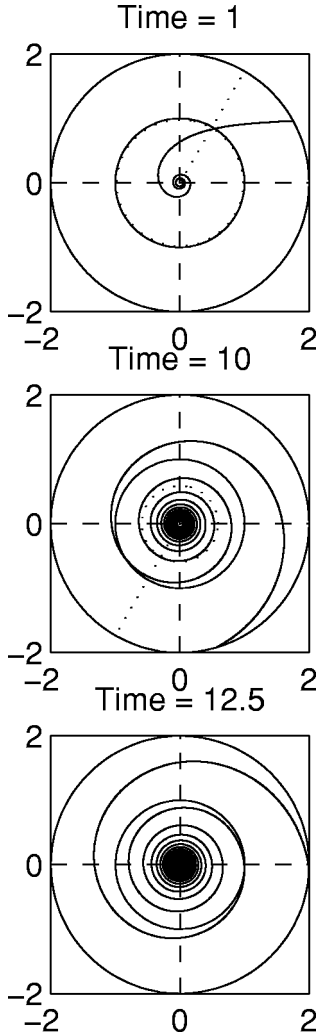


FIG. 2. Representation of the maximum probability position as the intersection of the spiral S and the circle of radius r_p . The Reynolds number is $1/\nu=50$; times are $t=1, 10$, and 12.5 . The radius of the dotted circle at each time: $r=r_p=0.98, 0.59$, and 0.09 ; solid circle: $r=r_0=1$; dotted line: $\theta=\theta_p$.

study of the spiral structure. In Fig. 2 the spiral S is plotted at three different times. We choose the Reynolds number $\text{Re}=1/\nu=50$ in such a way as to observe the merging of two vortices during a valid approximation time. At the beginning, $t=1$, the distance distribution is closely concentrated around $r_p(1)\sim 0.98\sim 1$: the two vortices have mutually rotated by $\theta_p\sim\pi/3$ but their distance is practically the initial one [see formula (4.28)]. The vortices are still clearly separated. The coupling effects between rotation and diffusion are still negligible. Therefore, at short times the vorticity distribution corresponds to two well separated Lamb vortices subject to rotation ($\Gamma\neq 0$).

At time $t=10$, $r_p\sim 0.59$ and $\theta_p\sim 4\pi/3$. The distance distribution is essentially concentrated on the spiral with radial values $r\in[r_p-(\nu t)^{1/2}, r_p+(\nu t)^{1/2}]$, that is to say angular values $\theta\in[2\pi+1.6\pi, 10\pi+1.5\pi]$: this corresponds to the development and stretching of vortex arms, which wind around the other vortex. Here each arm winds the other vortex on several rotations.

After this transitory period, r_p quickly decreases and at $t=12.5$, $r_p\sim 0.09$: the spiral is tightly bounded around r_p [as can also be seen from formula (4.29)], and becomes similar to circles. At this time the angular isotropy is fully developed, Θ is almost uniform in the region where the probability is concentrated, showing the disappearance of the spiral arms, and the merging is ending. Finally, $r_p\sim 0$, and the further evolution is purely diffusive.

One may distinguish two different regimes of the merging process. One is dominated by rotation, and the other is dominated by viscosity. The distinction between these two regimes depends on the values of the Reynolds number $1/\nu$ [also see Eq. (4.28)]. Let us compute the spiral step Δr for short times. Using $\theta(t)\approx t/r(t)$ and $r(t)\approx 1-\nu t/2$, one obtains $\Delta r\approx \pi\nu/(1+\pi\nu)$. Therefore, when $\nu\rightarrow\infty$ the spiral is initially very close to a circle (the deterministic motion), and the probability distribution will concentrate in a ring. In the opposite limit $\nu\rightarrow 0$, the spiral step tends to 1, the initial distance between the vortices, and the probability will quickly concentrate on the center: the two vortices merge before completing a rotation.

An intuitive visualization of the merging process is provided by the evolution of the probability distribution. Instead of using an exact formula, this distribution can be computed by numerically integrating the Langevin equation for a large number of independent particles, initially placed at a distance $r(0)=r_0=1$. Plotting the histogram of their positions at different times, one obtains a representation of the mean vorticity distribution. Figure 3 illustrates the two regimes of the merging process, in Fig. 3(a) we show the two vortex merging with the parameters used in Fig. 2. We see that before merging the two vortices form a ring structure (not perfectly circular) which progressively shrinks into the center. In Fig. 3(b) we show the limit of small Reynolds number (we take $1/\nu=8$), when there is no formation of the ring before the vortex merge. In this case the vortices collide following an open spiral trajectory. Another interesting effect observable in both cases is the differential rotation of the vortex distribution. Indeed, the central parts of the vortices have different orientations than their periphery, showing that the spiral trajectory is not followed at constant velocity; when the vortices approach each other, they accelerate.

The asymptotic regime discovered by Lundgren [8] is relevant in the time range $\nu^{-1/3}\ll t\ll\nu^{-1/2}$. The nonaxisymmetric structure of the distance between vortices probability density decays in a time much shorter than the viscous time. This prediction is in accordance with the formation of the ‘‘ring’’ vorticity distribution before the appearance of a pure diffusion dominated regime. For $1/\nu=50$ the time interval is $t\in(3.7, 7)$, the (maximum) radial diffusion can be estimated as $\Delta r=2\sqrt{\nu t}\sim\nu^{1/4}\approx 0.7$, while for $1/\nu=8$, $t\in(2.2, 2.8)$, it becomes $\Delta r\approx 1.2$ —larger than the initial vortex distance. These values are consistent with the simulations in Fig. 3, and agree with the prediction of a faster decay of the nonaxisymmetric harmonics.

V. PROBABILISTIC NATURE OF THE EXACT SOLUTION

First we show that solution (3.24) is defined in the sense that this is a normally (and therefore simply) convergent se-

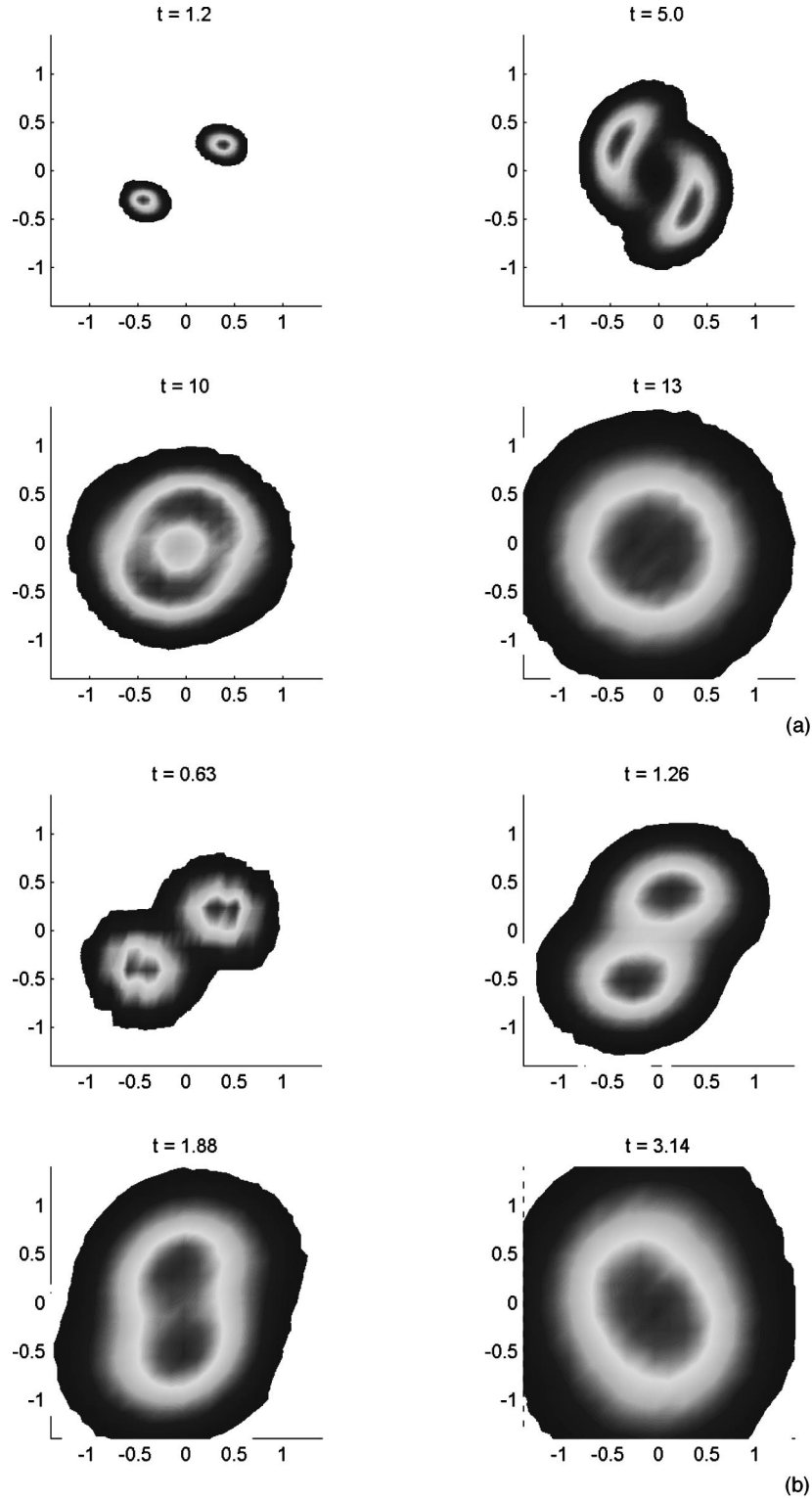


FIG. 3. Histogram of the vortex positions computed from the Langevin equations of the two point vortex system. Levels grow from black to white and from white to gray. (a) $N=100\,000$ pairs of vortices at $t=1.2, 5, 10,$ and 13 for $1/\nu=50$. (b) $N=200\,000$ pairs of vortices at $t=0.63, 1.26, 1.88,$ and 3.14 for $1/\nu=8$.

ries. Then we verify that this is effectively a probability distribution.

Concerning the convergence, it is sufficient to show that when $p \rightarrow +\infty$, $|\mu_p| \sim p$, and therefore $|I_{\mu_p}(x)| \sim I_p(x)$ for any positive x . By noting that

$$\left| I_0\left(\frac{r}{2\nu t}\right) + 2\Re \sum_{p=1}^{+\infty} I_{\mu_p}\left(\frac{r}{2\nu t}\right) e^{ip\theta} \right| \leq \left| I_0\left(\frac{r}{2\nu t}\right) \right| + 2 \sum_{p=1}^{+\infty} \left| I_{\mu_p}\left(\frac{r}{2\nu t}\right) \right|, \tag{5.1}$$

the normal convergence is a direct consequence of the convergence of the positive series

$$I_0(x) + 2 \sum_{p=1}^{+\infty} I_p(x) = \exp(x) \quad \text{for } x > 0. \quad (5.2)$$

The conservation of the total probability with the time comes from (see formula 6.633 in Ref. [27])

$$\begin{aligned} & \int_{r=0}^{+\infty} \int_{\theta=0}^{2\pi} P(r, \theta, t) r dr d\theta \\ &= 2\pi \int_{r=0}^{+\infty} r dr \frac{1}{4\pi\nu t} e^{-(r^2+1)/4\nu t} I_0\left(\frac{r}{2\nu t}\right) \\ &= 1, \end{aligned} \quad (5.3)$$

because the nonzero Fourier modes ($p \neq 0$) vanish after the angular integration. Note that the Fokker-Planck equation (3.9) implies the conservation of the measure $\int P(\mathbf{r}, t) d\mathbf{r}$ with time. The integral we computed in Eq. (5.3) is just a verification of this property. Its numerical value, 1, agrees with the initial condition which trivially satisfies $\int P(\mathbf{r}, 0) d\mathbf{r} = 1$.

Now, to complete, we check that P is positive everywhere. By construction, P is real. Moreover if P is positive at a strictly positive time t_1 , then it is positive at any time t_2 . Indeed, the same similarity ratio $r/(2\nu t)$ appears in all the Fourier components of solution (3.24), and therefore

$$\forall (t_2 > 0), \forall (r_2 > 0), \exists (r_1 > 0): \frac{r_1}{2\nu t_1} = \frac{r_2}{2\nu t_2}. \quad (5.4)$$

Now, by using that $I_\mu(0) = 0$ for any nonzero subscript μ , in the limit $t \rightarrow +\infty$ (for a fixed position r) we find that the only dominant mode is the zero one, which is strictly positive [$I_0(0) = 1$]. To proceed to a rigorous derivation of this last point, we use a general property of series functions which states that, given two positive function series $[f_n(x)]_{n \in I}$ and $[g_n(x)]_{n \in I}$ (I countable),

- (i) $\forall n \in I, \lim_{x \rightarrow 0} f_n(x) = 0$,
- (ii) $\forall n \in I, f_n(x) \sim g_n(x),$
 $x=0$

then $\lim_{x \rightarrow 0} \sum_n f_n(x) = 0 \Rightarrow \lim_{x \rightarrow 0} \sum_n g_n(x) = 0$.

To show that Eq. (3.24) is positive in this limit, we just have to verify that $\sum_{p=1}^{+\infty} |I_{\mu_p}(x)|$ goes to zero when $x \rightarrow 0$. We have the relation

$$I_{\mu_p} \underset{x \rightarrow 0}{\sim} \frac{1}{\Gamma(\mu_p)} \left(\frac{x}{2}\right)^{\mu_p}, \quad (5.5)$$

where Γ is the gamma function. Let us now combine the Stirling formula

$$\Gamma(a) \underset{|a| \rightarrow +\infty}{\sim} \sqrt{2\pi} \exp[-a + (a-1/2)\ln a] \quad (5.6)$$

with the properties (i) $p \sim |\mu_p| \leq p$ and (ii) $\arg \mu_p$ which are bounded and converge to 0. They imply that $\cos(\arg \mu_p)$ converges to 1, and for p large enough,

$$\begin{aligned} & |\mu_p| \cos(\arg \mu_p) [-1 + \ln |\mu_p|] \\ & \sim p [\ln p - 1] \cos(\arg \mu_p) > p \ln p / 2 \end{aligned} \quad (5.7)$$

and

$$\begin{aligned} |\Gamma(\mu_p)| & \underset{p \rightarrow +\infty}{\sim} \sqrt{2\pi} e^{|\mu_p| \cos(\arg \mu_p) [-1 + \ln |\mu_p|] - |\mu_p| \sin(\arg \mu_p) \arg \mu_p} \\ & > e^{p \ln p / 2}. \end{aligned} \quad (5.8)$$

It follows that $\lim_{p \rightarrow +\infty} |\Gamma(\mu_p)| = +\infty$, and for p large enough,

$$\begin{aligned} I_{\mu_p}(x) & \underset{|p| \rightarrow +\infty}{\sim} \left| \frac{1}{\Gamma(\mu_p)} \left(\frac{x}{2}\right)^{\mu_p} \right| \leq |x^{\mu_p}| \\ & = \exp(|\mu_p| \cos(\arg \mu_p) \ln |x^{\mu_p}|) \leq x^{p/2}. \end{aligned} \quad (5.9)$$

By applying the series functions proposition stated above to relations (5.9), we can conclude that $\sum_{p=1}^{+\infty} |I_{\mu_p}(x)|$ converges. This result implies that P is positive at large times. It follows that Eq. (3.24) is a probability distribution.

One may also note that the asymptotic regime ($t \rightarrow +\infty$) is purely diffusive (diffusion of the radial distance between the two vortices) because

$$P(r, \theta, t) \sim \frac{1}{4\pi\nu t} e^{(r^2+1)/4\nu t} I_0\left(\frac{r}{2\nu t}\right), \quad (5.10)$$

which corresponds to the solution of a diffusion equation with initially, the probability concentrated in a ring of radius 1.

VI. CONCLUSION

In this paper, we have investigated some aspects of the dynamics of a finite number of point vortices in a viscous medium. Point vortices are well-studied solutions of Euler equations. Viscosity is introduced by inserting independent white noise perturbations into a point vortex Euler velocity field with a variance proportional to the viscosity itself. We have shown that the dynamics is a solution, in stochastic means, of the Navier-Stokes equations. It can be characterized by computing the probability distribution of their positions, which satisfy a Fokker-Planck equation.

In order to study the impact of the viscosity on the dynamics of point vortices, we focused on the simplest non-trivial case, which allowed us to describe the nondiffusive effects of the viscosity. The natural candidate was the system composed by two Lamb vortices. We analytically computed the probability distribution function solution of the Fokker-Planck equation in the special case where the two vortices have the same circulation. We verified that it is effectively a positive probability distribution.

This allowed us to show and describe in detail the merging process of the two Lamb vortices. This merging is a

nondiffusive viscous effect, and corresponds to a modification of the topology of the system. We also obtained that, in the limit $\nu t/r_0^2 \rightarrow 0$, the distribution of the distance between the two vortices is concentrated on a spiral structure. This characterizes the selection process, by viscosity, of a particular solution among an infinity of candidates at $\nu=0$. An important point in our asymptotic development is that it preserves the probabilistic character of the full solution, allowing a consistent interpretation of the analytical results. We also showed that corrections to the main contribution, in such a limit, are multipolar and preserve the topological nature (spiral geometry) of the selected solution. In fact, the sharp maximum of the distribution is located on this spiral structure. After a transitory regime (merging process), this maximum decreases exponentially to zero and angular isotropy follows. The asymptotic regime ($t \rightarrow \infty$) is purely diffusive and axisymmetric. We compared these asymptotic results with the exact ones using direct numerical simulations of the original Langevin equations. We verified, in particular, that the finite merging time of the two vortices, predicted analytically, corresponds to the one obtained in the simulations.

The complexity of the merging process manifests itself in an exact solution [Eq. (3.24)] by the presence and the combination of two time scalings: a purely diffusive one, where lengths scale as $r \sim \sqrt{\nu t}$; and a kinematic one, where lengths scale as $r \sim \Gamma/r_0 t$. At variance to the diffusive law, the kinematic relation depends on the total circulation, and more in-

terestingly, on the *initial* distance between the two vortices. The interplay of the two behaviors appears clearly in the expression of the fusion time (the time for which $r_p=0$) when written in terms of the dimensional variables $t_f = (r_0^2/8\nu)$. The typical diffusion time is r_0^2/ν , and one sees that the kinematic effect appears through the value of the numerical constant 1/8, which gives a fusion time much smaller than the diffusive one.

According to the value of the Reynolds number, we found two regimes of fusion of the two Lamb vortices. On the one hand, when kinematic effects are dominant, the merging process evolves through two stages: in the first one, angular diffusion dominates, and a ring is formed; in the second one, this ring shrinks toward the center, rapidly losing its asymmetric features. On the other hand, when the viscous effects are dominant, the vortices (in the sense of the averaged vorticity given by the probability distribution) remain relatively localized around two peaks, which directly collide to form a unique structure. This single peaked structure evolves rapidly to an axisymmetric one: a final Gaussian vortex, which is an asymptotic state independent of the initial condition and parameter values.

ACKNOWLEDGMENTS

We acknowledge interesting discussions with P.-H. Chavanis, S. Le Dizès, T. Leweke, and M. Rossi.

-
- [1] J. C. McWilliams, *J. Fluid Mech.* **146**, 21 (1984).
 - [2] G. F. Carnevale, J. C. McWilliams, Y. Pomeau, J. B. Weiss, and W. R. Young, *Phys. Rev. Lett.* **66**, 2735 (1991).
 - [3] J. B. Weiss and J. C. McWilliams, *Phys. Fluids A* **5**, 608 (1993).
 - [4] D. G. Dritshel and D. W. Waugh, *Phys. Fluids A* **4**, 1737 (1992).
 - [5] D. W. Waugh, *Phys. Fluids A* **4**, 1745 (1992).
 - [6] P. Saffman, *Vortex Dynamics*, Cambridge Monographs on Mechanics and Applied Mathematics (Cambridge University Press, Cambridge, 1995).
 - [7] L. Ting and R. Klein, *Viscous Vortical Flows* (Springer-Verlag, Berlin, 1991).
 - [8] T. S. Lundgren, *Phys. Fluids*, **25**, 2193 (1982).
 - [9] T. S. Lundgren, *Phys. Fluids A* **5**, 1472 (1993).
 - [10] H. K. Moffatt, in *New Approaches and Concepts in Turbulence*, edited by T. Dracos and A. Tsinober (Birkhäuser, Basel, 1993), pp. 121–129.
 - [11] J. C. Vassilicos and J. G. Brasseur, *Phys. Rev. E* **54**, 467 (1996).
 - [12] J. R. Angilella and J. C. Vassilicos, *Phys. Rev. E* **59**, 5427 (1999).
 - [13] C. Marchioro and M. Pulvirenti, *Commun. Math. Phys.* **84**, 483 (1982).
 - [14] L. Kelvin, *Proc. R. Soc. Edimburg* **VI**, 94 (1867).
 - [15] A. J. Chorin, *J. Fluid Mech.* **57**, 785 (1973).
 - [16] C. Marchioro and M. Pulvirenti, *Mathematical Theory of Incompressible Nonviscous Fluids* (Springer-Verlag, New York, 1994).
 - [17] H. Lamb, *Hydrodynamics* (Cambridge University Press, Cambridge, 1932).
 - [18] O. Agullo and A. D. Verga, *Phys. Rev. Lett.* **78**, 2361 (1997).
 - [19] E. Novikov, *Zh. Eksp. Teor. Fiz.* **68**, 1868 (1975) [*Sov. Phys. JETP* **41**, 937 (1975)].
 - [20] H. Aref, *Annu. Rev. Fluid Mech.* **15**, 345 (1983).
 - [21] H. Helmholtz, *Crelles* **55**, 25 (1858).
 - [22] C. W. Gardiner, *Handbook of Stochastic Methods* (Springer-Verlag, Berlin, 1985).
 - [23] J. Zinn-Justin, *Quantum Field Theory and Critical Phenomena* (Oxford, University Press, Oxford, 1989).
 - [24] A. Verga (unpublished).
 - [25] P. Meunier, T. Leweke, and M. Abid, in *Advances in Turbulence VIII*, edited by C. Dopazo (CIMNE, Barcelona, 2000), pp. 15–18.
 - [26] I. I. Gihman and A. V. Skorohod, *Stochastic Differential Equations* (Springer-Verlag, Berlin, 1972).
 - [27] I. Gradshteyn and I. Ryzhik, *Table of Integrals, Series and Products* (Academic Press, Boston, 1994).
 - [28] H. Poincaré, *Les Méthodes Nouvelles de la Mécanique Céleste* (Gauthier-Villars, Paris, 1893), Chap. VIII, p. 1.
 - [29] J. P. Ramis, *Séries Divergentes et Théories Asymptotiques, Panoramas et Synthèses* (Société Mathématique de France, Paris, 1992).